Computers and Mathematics with Applications 104 (2021) 50–58

Contents lists available at ScienceDirect

Computers and Mathematics with Applications

www.elsevier.com/locate/camwa

Numerical calculation of extremal Steklov eigenvalues in 3D and 4D

Pedro R.S. Antunes *

Univ. Aberta, Dep. of Sciences and Technology, Rua da Escola Politécnica 141-7, P-1269-001 Lisboa, Portugal
Univ. Lisboa, Faculty of Sciences, Group of Mathematical Physics, Edifício 6, Piso 1, Campo Grande, P-1749-016 Lisboa, Portugal

ARTICLE INFO

Keywords:
Steklov eigenvalues
Shape optimization
Method of fundamental solutions

ABSTRACT

We develop a numerical method for solving shape optimization of functionals involving Steklov eigenvalues and apply it to the problem of maximization of the k-th Steklov eigenvalue, under volume constraint. A similar study in the planar case was already addressed in the literature using the boundary integral equation method. Here we extend that study to the 3D and 4D cases, using the Method of Fundamental Solutions as the forward solver.

1. Introduction

Let $\Omega \subset \mathbb{R}^d$ be a bounded open set and consider the second order Steklov eigenvalue problem,

$$\begin{cases} \Delta w = 0 & \text{in } \Omega \\ \frac{\partial w}{\partial n} = \sigma w & \text{on } \partial\Omega, \end{cases} \tag{1}$$

defined in $H^1(\Omega)$. We will denote the eigenvalues by $0 = \sigma_0(\Omega) \le \sigma_1(\Omega) \le \sigma_2(\Omega) \le \ldots \to \infty$ where each eigenvalue $\sigma_k(\Omega)$ is counted with its multiplicity and the corresponding orthonormal real eigenfunctions by $w_i,\ i = 0, 1, 2, \ldots$. The eigenvalues can also be defined through a variational characterization

$$\sigma_k(\Omega) = \min_{S \in \mathcal{S}_{k+1}} \max_{w \in S \setminus \{0\}} \frac{\int_\Omega |\nabla w|^2 dx}{\int_{\partial\Omega} w^2 ds_x}, \tag{2}$$

where $\mathcal{S}_{k+1}$ is the family of all subspaces of dimension $k+1$ in $H^1(\Omega)$ (e.g. [13]).

Some shape optimization problems for Steklov eigenvalues were already considered in the literature. For example, in [31] the author proved that the disk maximizes the first non trivial eigenvalue of the problem

$$\begin{cases} \Delta w = 0 & \text{in } \Omega \\ \frac{\partial w}{\partial n} = \sigma \rho w & \text{on } \partial\Omega, \end{cases} \tag{3}$$

among simply connected planar domains with a fixed mass $M(\Omega) = \int_{\partial\Omega} \rho ds_x$, where $\rho \ge 0$ is a $L^\infty(\partial\Omega)$ function on the boundary. The extension of this result to non simply connected domains is an open problem. For higher eigenvalues, in [22] the authors proved a result that implies the following inequality for simply connected planar domains,

$$\sup\left\{\sigma_k(\Omega) M(\Omega) :\ \Omega \subset \mathbb{R}^2\right\} \le 2\pi k, k \in \mathbb{N}. \tag{4}$$

In [21], it was proved that the previous inequality is sharp and attained by a sequence of simply connected domains degenerating into a disjoint union of k disks of the same area.

The connection of extremal Steklov eigenvalue problems and the problem of generating free boundary minimal surfaces in the Euclidean ball was studied in [20] and this connection was explored numerically in [27].

In this work, we will consider the following shape optimization problem

$$\sigma_k^\star = \max_{\Omega \subset \mathbb{R}^d} \left\{\sigma_k(\Omega),\ |\Omega| = 1\right\},\ k = 1, 2, \ldots. \tag{5}$$

where σ_k are the eigenvalues of problem (1) and taking into account the properties

$$\sigma_k(t\Omega) = \frac{1}{t}\sigma_k(\Omega),\ \forall t > 0$$

and

$$|t\Omega| = t^d |\Omega|,\ \forall t > 0$$

the problem (5) is equivalent to

Problem 1. *Given $k = 1, 2, \ldots$, determine*

$$\sigma_k^\star = \max_{\Omega \subset \mathbb{R}^d} \left\{\sigma_k(\Omega) |\Omega|^{1/d}\right\}.$$

The existence of an optimal set was proved in [13] and some numerical studies for the optimal solutions of this problem in 2D can be found

* Correspondence to: Univ. Aberta, Dep. of Sciences and Technology, Rua da Escola Politécnica 141-7, P-1269-001 Lisboa, Portugal.
E-mail address: prantunes@fc.ul.pt.

https://doi.org/10.1016/j.camwa.2021.11.008
Received 28 July 2021; Received in revised form 6 November 2021; Accepted 15 November 2021

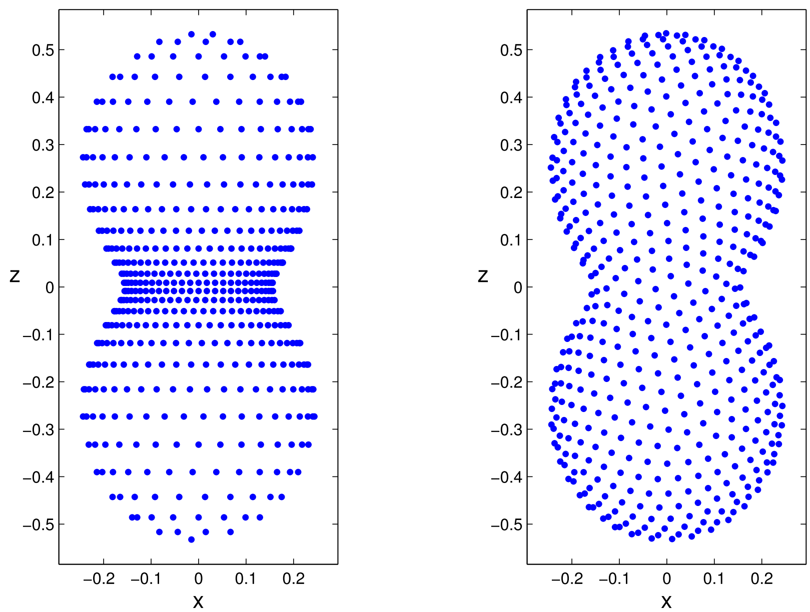

Fig. 1. Two distribution of points on the boundary of a star-shaped domain.

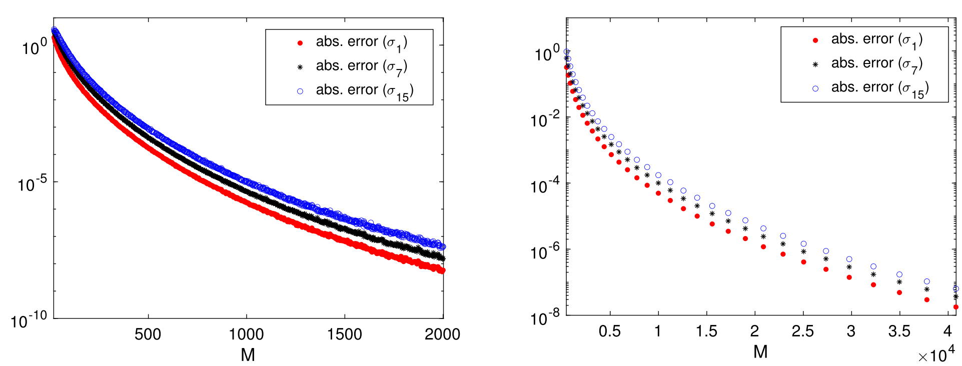

Fig. 2. Convergence curve for the MFS approximation of σ_k, $k = 1, 7, 15$ of the ball of unit volume in 3D (left plot) and 4D (right plot).

in [1,11,13]. As pointed out in [1], the optimal domains for this problem in 2D are well structured. In particular, the optimizer for σ_k seems to have k-fold symmetry and the corresponding optimal eigenvalue has multiplicity 2, if k is even and multiplicity 3, if $k \geq 3$ is odd. Also some progress on the analytical study of this problem has been made recently. In [29], using a perturbation argument the authors proved that the disk is not the maximizer for higher even numbered Steklov eigenvalues. In this work we will address a numerical study for the optimizers in 3D and 4D.

2. Shape derivatives

We will consider the numerical solution of Problem 1 using a gradient-type method. In this context it is convenient to make use of the formulas for the shape derivatives of Steklov. Consider an application $\Psi : t \in [0, T[\to W^{1,\infty}(\mathbb{R}^d, \mathbb{R}^d)$ for which $\Psi(t) = I + tV$, where $W^{1,\infty}(\mathbb{R}^d, \mathbb{R}^d)$ is the set of bounded Lipschitz maps from $\mathbb{R}^d$ into itself, I is the identity and V is a given deformation field.

We will use the notation $\Omega_t = \Psi(t)(\Omega)$ and $\sigma(t) := \sigma(\Omega_t)$ and we assume that $\sigma(0)$ is simple.

Define the function $\mathcal{V}(t) = |\Omega_t|$, which gives the volume of the domain Ω_t. Then the shape derivative of $\mathcal{V}$ is given by

$$\mathcal{V}'(0) = \int_{\partial\Omega} V.n\, ds_x. \tag{6}$$

The shape derivative for a Steklov eigenvalue, which can be found in [15,1], is given by

$$\sigma'(0) = \int_{\partial\Omega} \left(|\nabla w|^2 - 2\sigma^2 w^2 - \sigma \mathcal{H} w^2 \right) V.n ds_x,$$

where $\mathcal{H}$ is the mean curvature.

3. Numerical methods

In this section we describe briefly the numerical methods that were used to solve Problem 1.

3.1. Parametrization of the domains

For the numerical solution of the Problem 1, we assume that Ω is a star-shaped domain whose boundary can be parameterized by

$$\begin{cases} x = r(\theta, \phi) \sin(\theta) \cos(\phi) \\ y = r(\theta, \phi) \sin(\theta) \sin(\phi) \\ z = r(\theta, \phi) \cos(\theta) \end{cases} \tag{7}$$

with $r(\theta, \phi) > 0$ for $\theta \in [0, \pi]$ and $\phi \in [0, 2\pi[$, and

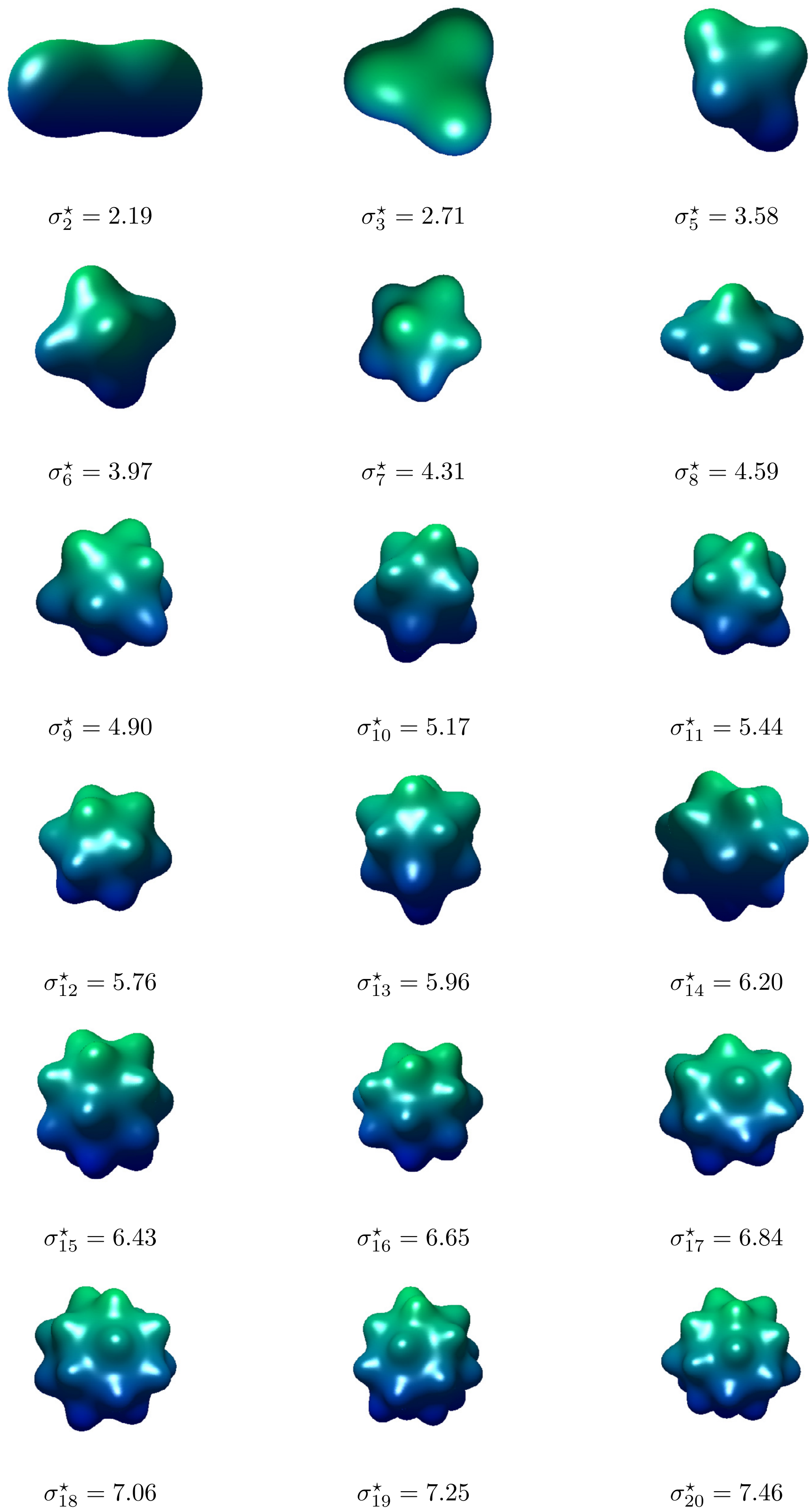

Fig. 3. Numerical optimizers and optimal eigenvalues obtained for Problem 1 in 3D. We obtained also the following optimal eigenvalue $\sigma_4^\star = 3.22$, whose optimizer is the ball.

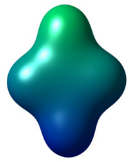

Fig. 4. Local maximizer of σ_4.

$$\begin{cases} x = r(\beta,\theta,\phi)\sin(\beta)\sin(\theta)\cos(\phi) \\ y = r(\beta,\theta,\phi)\sin(\beta)\sin(\theta)\sin(\phi) \\ z = r(\beta,\theta,\phi)\sin(\beta)\cos(\theta) \\ w = r(\beta,\theta,\phi)\cos(\beta) \end{cases} \tag{8}$$

where $r(\beta,\theta,\phi) > 0$, for $\beta \in [0,\pi]$, $\theta \in [0,\pi]$ and $\phi \in [0,2\pi[$, respectively for 3D and 4D domains.

We define the family of 3D spherical harmonics

$$S_l^m(\theta,\phi) = \begin{cases} \sqrt{2}k_l^m \cos(m\phi)P_l^m(\cos(\theta)) & \text{if } m > 0, \\ k_l^0 P_l^0(\cos(\theta)) & \text{if } m = 0, \\ \sqrt{2}k_l^m \sin(-m\phi)P_l^{-m}(\cos(\theta)) & \text{if } m < 0, \end{cases}$$

where P_l^m is an associated Legendre polynomial and

$$k_l^m = \sqrt{\frac{(2l+1)(l-|m|)!}{4\pi(l+|m|)!}}.$$

The 4D hyper-spherical harmonics are defined by

$$\begin{aligned} &S_{nl}^m(\beta,\theta,\phi) = c_{n,l,m}\sin^l(\beta)C_{n-l}^{l+1}(\cos(\beta))\,S_l^m(\theta,\phi)(\beta,\theta,\phi), \\ &n = 0,1,2,\ldots \quad \beta \in [0,\pi] \\ &0 \le l \le n \quad ,\ \theta \in [0,\pi] \quad , \\ &-l \le m \le l \quad \phi \in [0,2\pi[\end{aligned} \tag{9}$$

where S_l^m are 3D spherical harmonics, C_{n-l}^{l+1} are Gegenbauer polynomials and

$$c_{n,l,m} = 2^{l+\frac{1}{2}}\sqrt{\frac{(n+1)\Gamma(n-l+1)}{\pi\Gamma(n+l+2)}}\Gamma(l+1).$$

The function r is expanded in 3D and 4D respectively in terms of 3D spherical harmonics, for a fixed $N \in \mathbb{N}$,

$$r(\theta,\phi) = \sum_{l=0}^{N}\sum_{m=-l}^{l} a_{l,m}S_l^m(\theta,\phi), \tag{10}$$

and 4D hyper-spherical harmonics

$$r(\beta,\theta,\phi) = \sum_{n=0}^{N}\sum_{l=0}^{n}\sum_{m=-l}^{l} a_{n,l,m}S_{nl}^m(\beta,\theta,\phi) \tag{11}$$

and the optimization is performed by searching for optimal coefficients in these expansions.

3.2. Generation of points for the method of fundamental solutions

In [7] it was proposed a fast algorithm for the generation of points on the boundary of 3D and 4D star-shaped domain. It is based on an almost uniform distribution of points on the unitary sphere. Another numerical approach to obtain a quasi-equidistant point distribution over the surface of a sphere was proposed in [8]. The problem of distributing some points on a sphere in order to maximize the minimum distance between pairs of points is known as Tammes problem ([28,14]) and the optimal distribution was already found for some particular small numbers N (e.g. [19,16,25]).

The location of points on the boundary of a general star-shaped domain can be obtained directly from (8), mapping a sample of points almost uniformly distributed on the surface of the sphere to points on the boundary of the domain. However, we have the effect of the function r and in some cases this can generate clusters of nodes (see Fig. 1-left).

Another strategy is to calculate the points x_i, $i = 1,\ldots,N$ that minimize the Riesz energy,

$$E(N,s) = \sum_{1\le i<j\le N}\frac{1}{|x_i - x_j|^s}.$$

The Coulomb potential that models electrons repelling each other is the case $s = 1$. To illustrate the results obtained with both numerical algorithms we considered a 3D star-shaped domain parametrized by (7), where

$$r(\theta,\phi) = 1 + 0.4S_2^0(\theta,\phi).$$

In Fig. 1-left we plot 1000 points obtained with the distribution of points considered in [7]. Then, this distribution of points was improved by minimizing the Riesz energy, with $s = 3$ and we obtained the distribution of nodes of Fig. 1-right. This approach is much more expensive from the computational point of view, but provides a much better distribution of nodes. We considered an analogous algorithm for placing the nodes on the boundary of 4D domains. Before running the optimization procedure we calculate the vector of the angles that define the location of the points on the boundary of the initial guess, by minimizing Riesz energy. During the optimization procedure, after a few iterations we may observe some clusters in some parts of the boundary. Thus, after each 10 iterations of the eigenvalue optimization we refine the vector containing the angles that generate the collocation points by calculating a few iterations of the minimization of Riesz energy.

We will follow the choice for the source points of the MFS proposed in [2,3]. We take M_C collocation points x_i, $i = 1,\ldots,M_C$ almost uniformly distributed on the boundary of the domain obtained by using the algorithm described above and for each of these points we calculate the outward unitary vector n_i, which is normal to the boundary at x_i. The source points are defined by

$$y_i = x_i + \delta\, n_i,$$

where δ is a parameter chosen such that the source points remain outside $\bar{\Omega}$.

3.3. Numerical solution of the eigenvalue problems

The Steklov eigenvalue Problem 1 will be solved by the Method of Fundamental Solutions (MFS). We take the fundamental solution of the Laplace equation in $\mathbb{R}^d$, $d \ge 3$ (e.g. [17]),

$$\Phi(x) = \frac{1}{d(d-2)\alpha(d)|x|^{d-2}}, \tag{12}$$

where $\alpha(d)$ denotes the volume of the unit ball in $\mathbb{R}^d$.

The MFS approximation is a linear combination

$$u(x) \approx \tilde{u}(x) = \sum_{j=1}^{M}\beta_j\phi_j(x), \tag{13}$$

where

$$\phi_j = \Phi(\cdot - y_j) \tag{14}$$

are M point sources centered at some points y_j that are placed on an admissible source set $\hat{\Gamma}$, which is assumed to be the boundary of a bounded open set $\hat{\Omega}$ such that $\bar{\Omega} \subset \hat{\Omega}$, with $\hat{\Gamma}$ surrounding $\partial\Omega$. The MFS approximation (13) can be seen as a discretization of the single layer operator

$$\begin{aligned} &S : C(\hat{\Gamma}) \to C(\partial\Omega) \\ &(S\varphi)(x) = \int_{\hat{\Gamma}} \Phi(x-y)\varphi(y)ds_y \end{aligned}$$

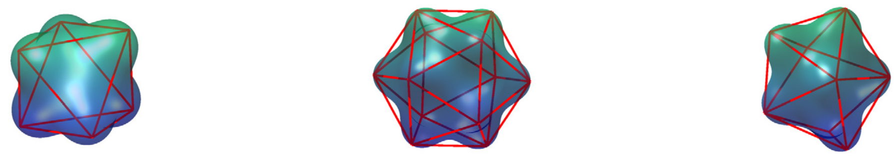

(a) (b) (c)

Fig. 5. (a) Maximizer of σ_6 and an octahedron; (b) Maximizer of σ_{20} and an icosahedron; (c) Maximizer of σ_8 and the *corresponding* polyhedron, which is not a Platonic solid.

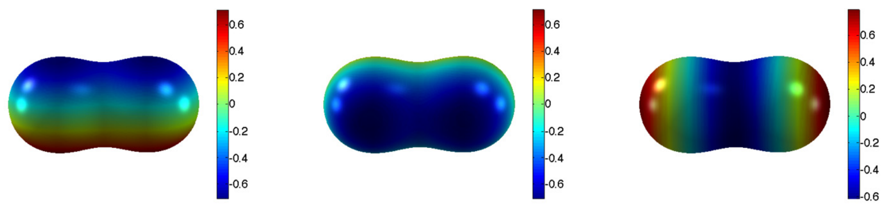

Fig. 6. Eigenfunctions associated to the optimal eigenvalue σ_2.

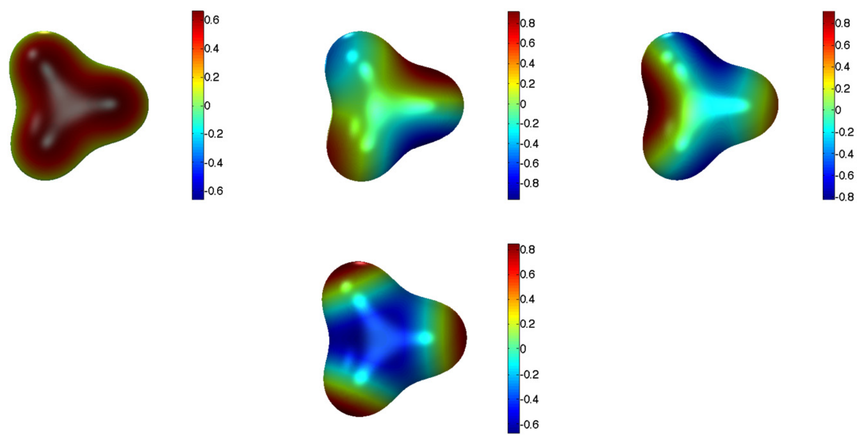

Fig. 7. Eigenfunctions associated to the optimal eigenvalue σ_3.

which is known to be injective, for $d > 2$ (e.g. [23]). By construction, the MFS approximation satisfies the Laplace equation because it is built using shifts of the fundamental solution. Moreover, since it is a mesh and integration free method it is particularly suitable to deal with boundary value problems defined in 3D or 4D domains, as those considered in this paper. For more details about the MFS, we refer to the following works [24,10,18,2,9,3,4,12,5].

The approximation of the Steklov eigenvalues can be calculated by solving generalized matrix eigenvalue problems. We define the matrices **A** and **B**, where

$$(\mathbf{A})_{i,j} = \partial_{n_i}\Phi(x_i - y_j) \quad (\mathbf{B})_{i,j} = \Phi(x_i - y_j).$$

The eigenvalues are calculated by solving the generalized matrix eigenvalue problem

$$\mathbf{A}X = \Lambda\mathbf{B}X$$

using the Matlab routine `eigs`.

Next, we test our algorithm for the calculation of Steklov eigenvalues in the case of 3D and 4D balls, for which we know the exact solutions. Fig. 2 shows the absolute error of the approximations for three eigenvalues, σ_1, σ_7 and σ_{15} in 3D (left plot) and 4D (right plot), which were obtained for $\delta = 0.2$.

3.4. Optimization algorithm

We define $\mathcal{V} \in \mathbb{R}^P$ to be the vector of all the coefficients in the linear combinations (10) and (11). Then, we define the cost function

$$\mathcal{C}_k(\mathcal{V}) := \sigma_k(\Omega)|\Omega|^{\frac{1}{d}},$$

where Ω is the domain whose boundary is obtained from $\mathcal{V}$, by using (10) and (11) and will denote by $\mathcal{V}_k^*$ optimal coefficients defining a maximizer of σ_k. The numerical maximization of the functional $\mathcal{C}_k$ may be difficult, in the sense that it is expected that the optimizers may have eigenvalues with large multiplicities,

$$\mathcal{C}_k(\mathcal{V}_k^*) = \mathcal{C}_{k+1}(\mathcal{V}_k^*) = \ldots = \mathcal{C}_{k+\mathcal{M}-1}(\mathcal{V}_k^*),$$

for some $\mathcal{M} \geq 1$ defining the multiplicity of the optimal eigenvalue.

Thus, we must solve highly non-smooth optimizations. Several numerical approaches were proposed in the literature to deal with non-smoothness of the objective function in the optimization of eigenvalues (e.g. [26,6,7,1]). Here, we propose to use a gradient type method, with a convenient choice of the direction for performing a line search. We will assume that, due to numerical errors, all the domains that considered in the optimization procedure have simple eigenvalues and thus, we can calculate the gradients $g_k, g_{k+1}, \ldots, g_{k+\mathcal{M}-1}$ corresponding respectively to $\mathcal{C}_k, \mathcal{C}_{k+1}, \ldots, \mathcal{C}_{k+\mathcal{M}-1}$.

A typical situation during the optimization procedure is to obtain a certain domain having a few eigenvalues which are very close to each

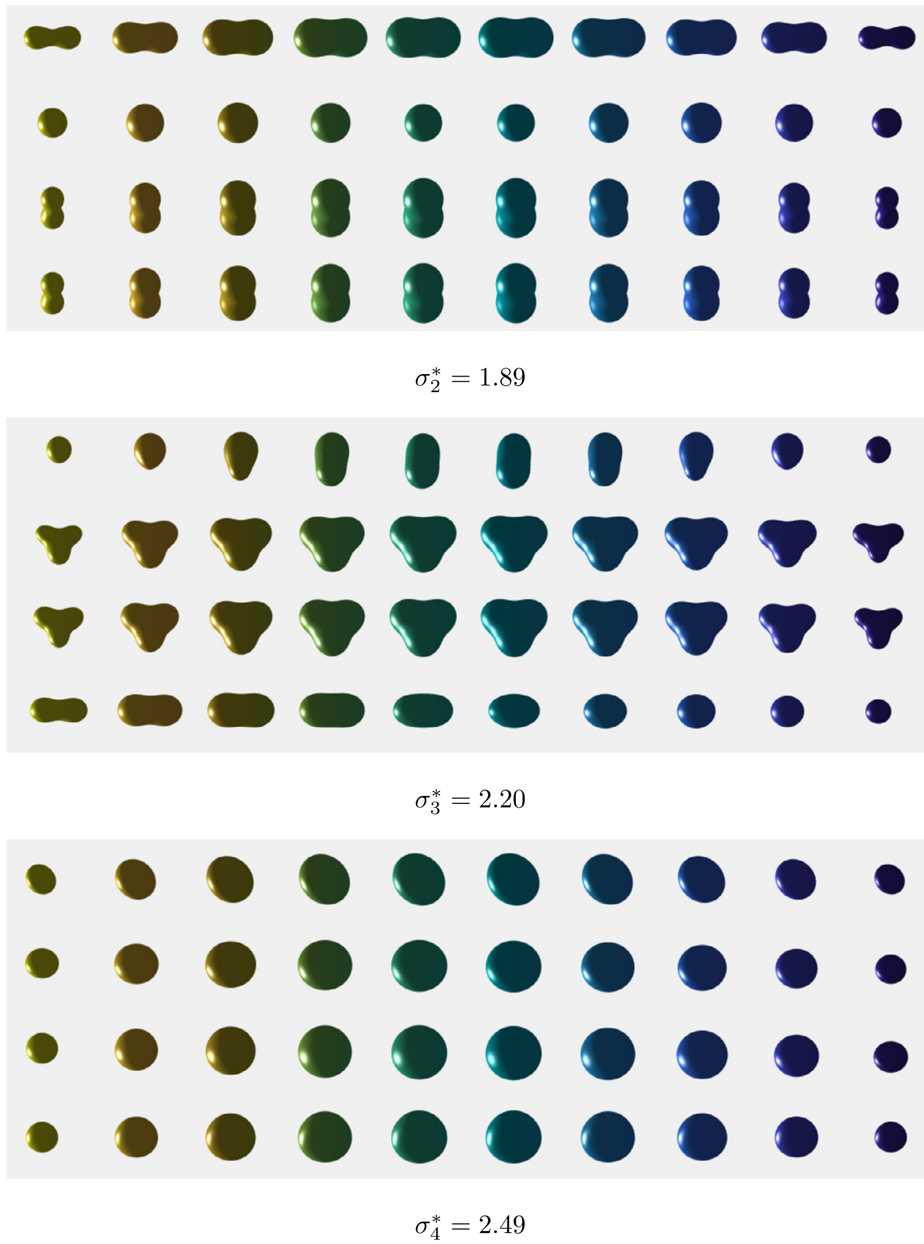

Fig. 8. Orthogonal cuts of the optimizers of σ_k, $k = 2, 3, 4$ in 4D.

other and we would like the algorithm to increase all of them. To be more precise, let's assume that we define a small threshold parameter ϵ and that at some iteration, for some $\mathcal{M} \geq 1$, we obtain

$$C_{k+\mathcal{M}}(\mathcal{V}) - C_k(\mathcal{V}) \leq \epsilon, \text{ but } C_{k+\mathcal{M}+1}(\mathcal{V}) - C_k(\mathcal{V}) > \epsilon$$

The ascent direction will be determined by solving the max min problem

$$\hat{v} = \max_{v \in \mathbb{R}^P : \|v\|=1} \min \left(g_k \cdot v, g_{k+1} \cdot v, ..., g_{k+\mathcal{M}-1} \cdot v \right). \tag{15}$$

Note that from the computational point of view, the numerical solution of problem (15) is not expensive, when compared to the calculation of the eigenvalues and gradients.

4. Numerical results and discussion

In this section we present some numerical results that we obtained for the solution of Problem 1. In all the experiments, we took N = 20 for the parametrization of 3D and 4D domains, through functions r defined in (10) and (11) and the Steklov eigenvalues and eigenfunctions were calculated with 2000 and 8000 collocation points, respectively in 3D and 4D, taking $\delta = 0.2$ in both cases. The calculation of the optimal solutions of Problem 1 requires approximately 50 and 100 iterations, respectively in 3D and 4D, taking around one hour for 3D problems, while the 4D problems may require 10 hours of computation using Matlab 2020a on a 2,8 GHz quad-core Intel Core i7 with 16 GB of RAM.

Fig. 3 shows optimizers of Problem 1 among three dimensional geometries for $k = 2, 3, ..., 20$. The optimal eigenvalue is also marked in the Figure. All the values that are presented were obtained rounding down the optimal value obtained with our algorithm and are thus lower bounds for the optimal value. We can observe that, in a similar way that was obtained in the planar case in [1], in general the optimizers are well structured and have an increasing number of *buds*. Indeed, the maximizer of σ_k seems to have k buds. However, there are some ex-

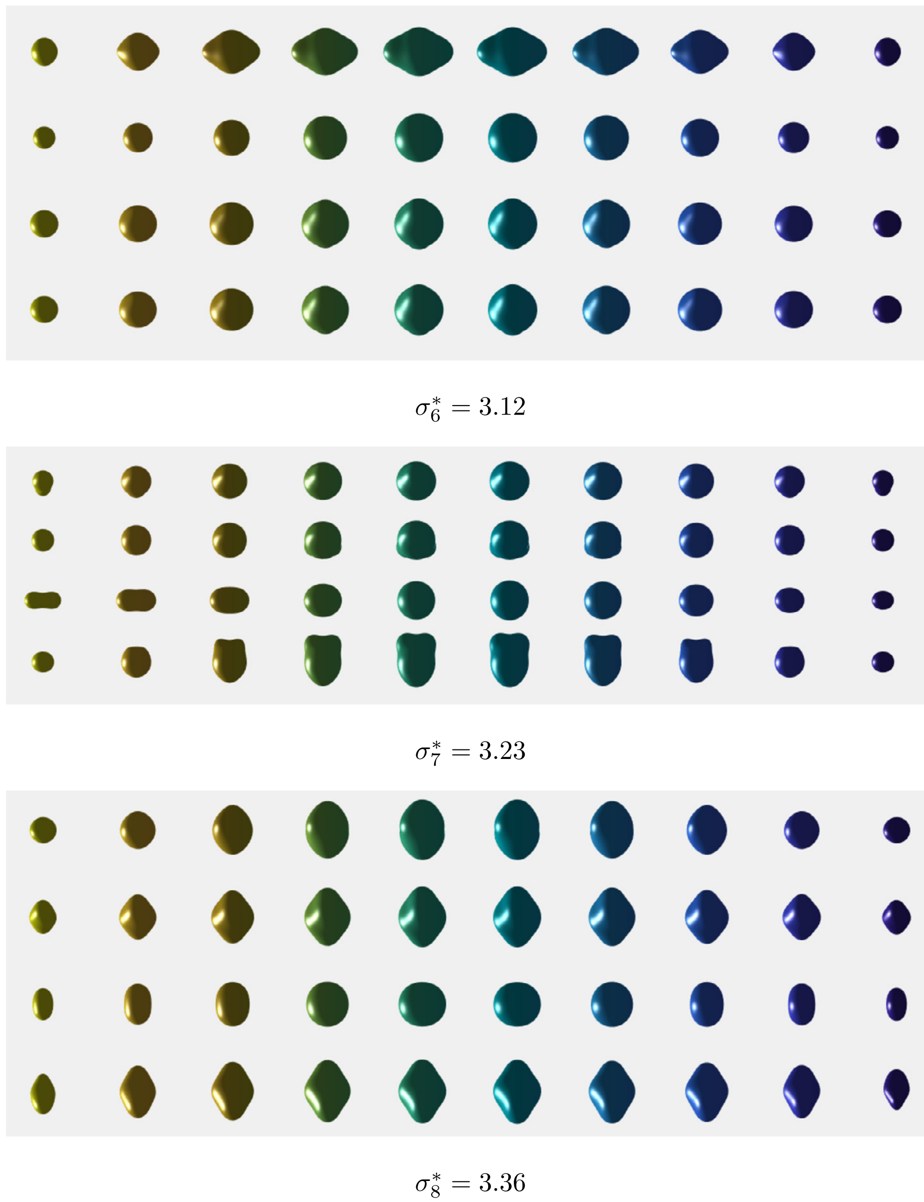

Fig. 9. Orthogonal cuts of the optimizers of σ_k, $k = 6, 7, 8$ in 4D.

ceptions in this pattern. We obtained a local maximizer for σ_4, that is plotted in Fig. 4, for which we obtain $\sigma_4 \approx 3.08$, but this eigenvalue is smaller than the corresponding eigenvalue of the ball. Depending on the initial guess for the optimization, our algorithm converges either to the domain plotted in Fig. 4 or to the ball. Note that the volume-normalized Steklov eigenvalue σ_{p^2}, $p \in \mathbb{N}$ is stationary for the ball, as recently proved in [30]. This result could suggest the ball as a natural candidate for maximizer of σ_{p^2}, for $p \in \mathbb{N}$. Our numerical results suggest that ball maximizes σ_4 (corresponding to $p = 2$) but it is not the case when $p = 3$ or $p = 4$, for which we were able to find domains with eigenvalues larger than those of the ball, as shown in Table 1.

Some of the optimizers seem to have some symmetries and some of them can be related with Platonic solids. For instance, the optimizers of σ_6 and σ_{20} seem to have the same symmetries (and same number of vertices) of the octahedron and the icosahedron, respectively, as illustrated in Fig. 5 (a) and (b). However, some other optimizers have different properties. For example, there are Platonic solids having 8 and 20 vertices, which are the cube and the dodecahedron. The optimizers of σ_8 and σ_{20} do not have the same symmetries of these Platonic solids. Fig. 5 (c) shows the optimizer of λ_8 and a *corresponding* polyhedron, which is not a cube.

All the optimizers that we obtained have multiple optimal eigenvalues. For example the optimizer of σ_2 and σ_3 correspond to optimal eigenvalues with multiplicity three and four, respectively. In Figs. 6 and 7 we plot linear independent eigenfunctions associated to the optimal eigenvalue in both cases.

Next, we show similar results obtained in 4D. Note that in this case is not trivial how to represent the optimizers. We used an algorithm proposed in [7] that applies suitable rigid transformations to the optimizers obtained from the optimization procedure, in order to exhibit its symmetries (see [7] for details). Figs. 8, 9 and 10 show some 3D cuts of the optimizers in 4D in four orthogonal directions, for the optimizers of σ_k, $k = 2, \ldots, 10$. Every row in each picture corresponds to cuts in each of the four orthogonal directions. The optimal eigenvalues that were obtained are also presented at the Figure. The numerical results that we gathered suggest that the optimizer of σ_5 is the ball, for which we obtained $\sigma_5^* = 3.01$. Table 2 shows the optimal eigenvalues, together with the corresponding multiplicity. We included at the same Table the corresponding values of the ball.

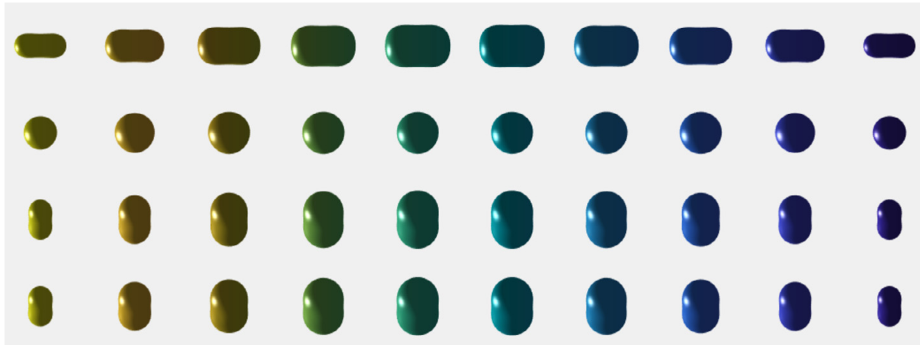

$\sigma_9^* = 3.60$

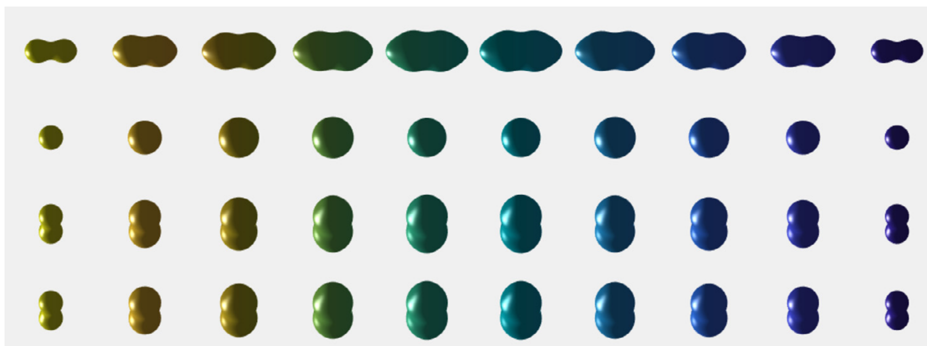

$\sigma_{10}^* = 3.71$

Fig. 10. Orthogonal cuts of the optimizers of σ_k, $k = 9, 10$ in 4D.

Table 1
Eigenvalues of the ball, optimal eigenvalues and multiplicities in 3D.

Eigenvalue of the ball	Optimal eigenvalue	Multiplicity
$\sigma_2 = 1.61$	$\sigma_2^\star = 2.19$	3
$\sigma_3 = 1.61$	$\sigma_3^\star = 2.71$	4
$\sigma_4 = 3.22$	$\sigma_4^\star = 3.22$	5
$\sigma_5 = 3.22$	$\sigma_5^\star = 3.58$	5
$\sigma_6 = 3.22$	$\sigma_6^\star = 3.97$	6
$\sigma_7 = 3.22$	$\sigma_7^\star = 4.31$	7
$\sigma_8 = 3.22$	$\sigma_8^\star = 4.59$	6
$\sigma_9 = 4.83$	$\sigma_9^\star = 4.90$	6
$\sigma_{10} = 4.83$	$\sigma_{10}^\star = 5.17$	7
$\sigma_{11} = 4.83$	$\sigma_{11}^\star = 5.44$	7
$\sigma_{12} = 4.83$	$\sigma_{12}^\star = 5.76$	9
$\sigma_{13} = 4.83$	$\sigma_{13}^\star = 5.96$	8
$\sigma_{14} = 4.83$	$\sigma_{14}^\star = 6.20$	7
$\sigma_{15} = 4.83$	$\sigma_{15}^\star = 6.43$	9
$\sigma_{16} = 6.44$	$\sigma_{16}^\star = 6.65$	8
$\sigma_{17} = 6.44$	$\sigma_{17}^\star = 6.84$	7
$\sigma_{18} = 6.44$	$\sigma_{18}^\star = 7.06$	8
$\sigma_{19} = 6.44$	$\sigma_{19}^\star = 7.25$	7
$\sigma_{20} = 6.44$	$\sigma_{20}^\star = 7.46$	7

Table 2
Eigenvalue of the ball, optimal eigenvalues and multiplicities in 4D.

Eigenvalue of the ball	Optimal eigenvalue	Multiplicity
$\sigma_2 = 1.49$	$\sigma_2^\star = 1.89$	4
$\sigma_3 = 1.49$	$\sigma_3^\star = 2.20$	5
$\sigma_4 = 1.49$	$\sigma_4^\star = 2.49$	6
$\sigma_5 = 2.98$	$\sigma_5^\star = 3.01$	9
$\sigma_6 = 2.98$	$\sigma_6^\star = 3.12$	9
$\sigma_7 = 2.98$	$\sigma_7^\star = 3.23$	9
$\sigma_8 = 2.98$	$\sigma_8^\star = 3.36$	9
$\sigma_9 = 2.98$	$\sigma_9^\star = 3.60$	9
$\sigma_{10} = 2.98$	$\sigma_{10}^\star = 3.71$	9

References

[1] E. Akhmetgaliyev, C.-Y. Kao, B. Osting, Computational methods for extremal Steklov problems, SIAM J. Control Optim. 55 (2) (2017) 1226–1240.

[2] C.J.S. Alves, P.R.S. Antunes, The method of fundamental solutions applied to the calculation of eigenfrequencies and eigenmodes of 2D simply connected shapes, Comput. Mater. Continua 2 (4) (2005) 251–266.

[3] C.J.S. Alves, P.R.S. Antunes, The method of fundamental solutions applied to some inverse eigenproblems, SIAM J. Sci. Comput. 35 (3) (2013) A1689–A1708.

[4] P.R.S. Antunes, Numerical calculation of eigensolutions of 3D shapes using the method of fundamental solutions, Numer. Methods Partial Differ. Equ. 27 (6) (2011) 1525–1550.

[5] P.R.S. Antunes, A numerical algorithm to reduce the ill-conditioning in meshless methods for the Helmholtz equation, Numer. Algorithms 79 (3) (2018) 879–897.

[6] P.R.S. Antunes, P. Freitas, Numerical optimization of low eigenvalues of the Dirichlet and Neumann Laplacians, J. Optim. Theory Appl. 154 (2012) 235–257.

[7] P.R.S. Antunes, E. Oudet, Numerical minimization of Dirichlet-Laplacian eigenvalues of four-dimensional geometries, SIAM J. Sci. Comput. 39 (3) (2017) B508–B521.

[8] A. Araújo, P. Serranho, On the use of quasi-equidistant source points over the sphere surface for the method of fundamental solutions, J. Comput. Appl. Math. 359 (2019) 55–68.

[9] A.H. Barnett, T. Betcke, Stability and convergence of the method of fundamental solutions for Helmholtz problems on analytic domains, J. Comput. Phys. 227 (2008) 7003–7026.

[10] A. Bogomolny, Fundamental solutions method for elliptic boundary value problems, SIAM J. Numer. Anal. 22 (4) (1985) 644–669.

[11] B. Bogosel, The Steklov spectrum on moving domains, Appl. Math. Optim. 75 (1) (2015) 1–25.
[12] B. Bogosel, The method of fundamental solutions applied to boundary eigenvalue problems, J. Comput. Appl. Math. 306 (2016) 265–285.
[13] B. Bogosel, D. Bucur, A. Giacomini, Optimal shapes maximizing the Steklov eigenvalues, SIAM J. Math. Anal. 49 (2) (2017) 1645–1680.
[14] J.H. Conway, N.J.A. Sloane, Sphere Packings, Lattices and Groups, 2nd ed., Springer-Verlag, New York, 1993.
[15] M. Dambrine, D. Kateb, J. Lamboley, An extremal eigenvalue problem for the Wentzell–Laplace operator, Ann. Inst. Henri Poincaré, Anal. Non Linéaire 33 (2016) 409–450.
[16] L. Danzer, Finite point-sets on S^2 with minimum distance as large as possible, Discrete Math. 60 (1986) 3–66.
[17] L.C. Evans, Partial Differential Equations, Graduate Studies in Mathematics, vol. 19, AMS, Providence, 1991.
[18] G. Fairweather, A. Karageorghis, The method of fundamental solutions for elliptic boundary value problems, Adv. Comput. Math. 9 (1998) 69–95.
[19] L. Fejes Tóth, Über die Abschätzung des kürzesten Abstandes zweier Punkte eines auf einer Kugelfläche liegenden Punktsystems, Jber. Deutch. Math. Verein. 53 (1943) 66–68.
[20] A. Fraser, R. Schoen, The first Steklov eigenvalue, conformal geometry and minimal surfaces, Adv. Math. 226 (2011) 4011–4030.
[21] A. Girouard, I. Polterovich, On the Hersch-Payne-Schiffer estimates for the eigenvalues of the Steklov problem, Funct. Anal. Appl. 44 (2010) 106–117.
[22] J. Hersch, L.E. Payne, M.M. Schiffer, Some inequalities for Stekloff eigenvalues, Arch. Ration. Mech. Anal. 57 (1975) 99–114.
[23] R. Kress, Linear Integral Equations, 3rd edition, Springer, 2014.
[24] V.D. Kupradze, M.A. Aleksidze, The method of functional equations for the approximate solution of certain boundary value problems, USSR Comput. Math. Math. Phys. 4 (1964) 82–126.
[25] O.R. Musin, A.S. Tarasov, The Tammes problem for N = 14, Exp. Math. 24 (2015) 460–468.
[26] E. Oudet, Numerical minimization of eigenmodes of a membrane with respect to the domain, ESAIM Control Optim. Calc. Var. 10 (2004) 315–330.
[27] E. Oudet, C.-Y. Kao, B. Osting, Computation of free boundary minimal surfaces via extremal Steklov eigenvalue problems, ESAIM Control Optim. Calc. Var. 27 (2021) 34.
[28] R.M.L. Tammes, On the origin number and arrangement of the places of exits on the surface of pollengrains, Recl. Trav. Bot. Néerl. 27 (1930) 1–84.
[29] R. Viator, B. Osting, Steklov eigenvalues of reflection-symmetric nearly-circular planar domains, Proc. R. Soc. Lond., Ser. A, Math. Phys. Eng. Sci. (2018).
[30] R. Viator, B. Osting, Steklov eigenvalues of nearly spherical domains, arXiv:2104.03380, 2021.
[31] R. Weinstock, Inequalities for a classical eigenvalue problem, J. Ration. Mech. Anal. 3 (1954) 745–753.